RESPONSE OF COOLED PWO SCINTILLATORS TO LOW-ENERGY GAMMA-RAYS AND ITS IMPORTANCE FOR SPECTROSCOPIC MEASUREMENTS OF CHARMONIUM WITH PANDA*

D. Melnychuk, B. Zwieglinski

for the PANDA Collaboration at the FAIR Facility in Darmstadt

The Andrzej Sołtan Institute for Nuclear Studies
00-681 Warsaw, Hoża 69, Poland

(Received December 1, 2009)

Identification of π^0 and η mesons by detecting both γ-rays from their decay is a prerequisite for suppressing undesired background in studies of photon transitions between the states of charmonium. To achieve this goal the detection threshold of the PANDA electromagnetic calorimeter (EMC) should be as low as possible. We demonstrate with Monte-Carlo simulations how the signal to background ratio changes for the chosen $\bar{p}p \to h_c \to \gamma\eta_c$ reaction and the assumed exclusive η_c decay mode with the EMC threshold. The measurement of the h_c total width with a reasonable accuracy is feasible but time consuming in the high-resolution mode of HESR operation. Our PWO resolution measurement at low photon energies corroborates the trend established at the MAMI facility in the 40.9–674.5 MeV energy range.

PACS numbers: 25.70.Pq

1. Introduction

High precision charmonium spectroscopy is one of the major parts of the physics program for the PANDA experiment [1]. One may quote several examples from that program which require detection of high-energy photons, hence application of the PANDA Electromagnetic Calorimeter (EMC) [2]. Let us quote in the first instance the radiative transition between the 3526 MeV, $1^1P_1, h_c$ state and the ground state, $1^1S_0, \eta_c$, which is expected to be E1, based on the assumed quantum characteristics of the initial state

* Presented at the XXXI Mazurian Lakes Conference on Physics, Piaski, Poland, August 30–September 6, 2009.

and those assigned [3] to the final state. The expected quantum characteristics $J^{\mathrm{PC}} = 1^{+-}$ of h_c awaits establishing via measurement of the angular distribution of the γ, engaged in the transition, relative to the direction of the incident antiproton momentum. This will give firm foundation to expectation that the vector part in the potential models of the charm–anticharm interaction is weak [4]. Moreover, measurement of the partial E1 width of the $h_c \to \eta_c$ transition presents an independent interest to discriminate between different models for the quark wavefunctions and electromagnetic operators engaged in the transition, since the existing models differ strongly in their predictions (see Table I).

TABLE I

Partial and total width predictions for the h_c decay.

Author	Year	$\Gamma(\eta_c\gamma)$ (keV)	$\Gamma(J/\psi\pi^0)$ (keV)	$\Gamma(J/\psi\pi^0\pi^0)$ (keV)	Γ(hadrons) (keV)	Γ(tot) (keV)
Renard [5]	1976	240			370	500–1000
Novikov [6]	1977	975			60–350	
McClary [7]	1983	483				
Kuang [8]	1988		2	4.12	53.7	394
Chemtob [9]	1989		0.0061	52.6		
Galkin [10]	1990	559				
Bodwin [11]	1992	450			530	980
Casalbuoni [12]	1992	450				
Chao [13]	1992	385				
Chen [14]	1992		0.29–0.58	4.1–7.1	19–51	360
Ko [15]	1992	400	1.6			
Gupta [16]	1993	341.8				
Suzuki [17]	2002	520±90				
Lähde [18]	2003	661				
Barnes [19]	2005	498[a]				
		352[b]				
Dudek [20]	2006	663±132[c]				
		601±55[d]				
De Fazio [21]	2009	634±32				

[a]wavefunctions in nonrelativistic potential model,
[b]wavefunctions in relativized Godfrey–Isgur potential model,
[c]QCD lattice masses used,
[d]physical masses used.

2. Monte-Carlo studies of h_c detection with the PANDA detector

The offline software developed for the PANDA Physics Book [1] studies has been used in this analysis. It consists of several tools adapted from other HEP experiments which include event generators (EvtGen, DPM), particle tracking with GEANT4, digitization of the signal, reconstruction and identification of charged and neutral particles and high level analysis tools with vertex and kinematical fits.

2.1. Event selection and background suppression

The $h_c \to \eta_c + \gamma$ transition can be detected through many exclusive decay channels of η_c, neutral ($\eta_c \to \gamma\gamma$) or hadronic. The most promising decay mode of η_c from the point of view of the efficiency and signal to background ratio in detection with the PANDA detector appears $\eta_c \to \phi_1 + \phi_2$ with the branching ratio BR $= 2.6 \times 10^{-3}$. The background suppression for this decay mode was studied in order to demonstrate the detector performance. For the exclusive decay mode considered in this study:

$$\bar{p}p \to h_c \to \eta_c\gamma \to \phi\phi\gamma \to K^+K^-K^+K^-\gamma\,,$$

the following three reactions are considered as the main contributors to the background:

1. $\bar{p}p \to K^+K^-K^+K^-\pi^0\,,$
2. $\bar{p}p \to \phi K^+K^-\pi^0\,,$
3. $\bar{p}p \to \phi\phi\pi^0\,.$

Contributors 1–3 add to the background when one photon from the π^0 decay is left undetected, because then these reactions have the same final state particles as the studied h_c decay.

Fig. 1(a) presents the distributions of γs in the laboratory energy for the signal and the background channel 3. The energy range of γs from the h_c decay is practically within $[0.15; 2.0]$ GeV. The distribution for the background has different features. First, it is wider distributed extending beyond this energy range. Second, it has an increasing tendency towards zero energy. In order to recover π^0s to separate the signal from the background, one should succeed to lower photon detection threshold as much as possible.

Fig. 1(b) presents the multiplicity distribution of reconstructed EMC clusters for the signal and the background channels 3. One may note that the mean number of neutral candidates exceeds one, the value expected for the signal, or two expected for the background from π^0 decay. This is caused by hadronic split-offs, which make it impossible to select as the signal the events with only one cluster, because it leads to a significant drop in efficiency. This observation emphasizes the importance of other selection criteria, in particular of the veto on π^0 in an event. The effect of the latter requirement strongly depends on the assumed low energy photon threshold.

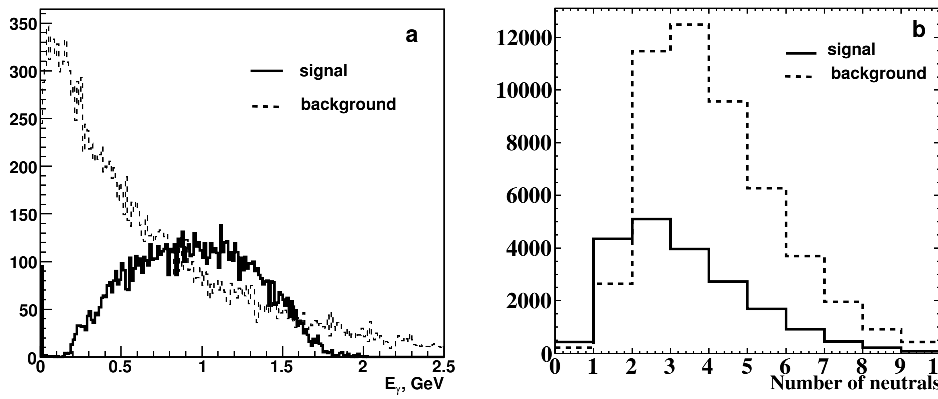

Fig. 1. Energy distribution of the γ for the $\bar{p}p \to h_c \to \eta_c\gamma$ and $\bar{p}p \to \phi\phi\pi^0$ reactions (a). The number of reconstructed EMC clusters for the $\bar{p}p \to h_c \to \eta_c\gamma$ and $\bar{p}p \to \phi\phi\pi^0$ reactions (b).

The following selection criteria were applied to the signal: a cut on the confidence level of the 4C-fit to beam energy momentum C.L. > 0.05, a cut on the η_c invariant mass [2.9;3.06] GeV, a cut on the ϕ invariant mass [0.99;1.05] GeV and a requirement that no π^0 is detected, *i.e.* all pairs of γs with the invariant mass in the range [0.115;0.15] GeV are rejected, the latter assuming two different low energy γ-ray thresholds: 10 and 30 MeV. The simulations performed for the $\bar{p}p \to \phi\phi\pi^0$ background channel demonstrated that the reduction of low energy γ-ray threshold from 30 MeV to 10 MeV gives about 20% improvement in the signal to background ratio, while for the $\bar{p}p \to \phi K^+K^-\pi^0$ the corresponding improvement is 40%. In the former case the signal selection efficiency is 24%. Assuming that HESR works in the high luminosity mode with $\mathcal{L} = 2 \times 10^{32}\mathrm{cm}^{-2}\mathrm{s}^{-1}$, the expected signal event rate is 92 events/day and the signal to background ratio is about 8.

2.2. Determination of the h_c total width

The total width of h_c is an important observable to be compared with those few estimates existing on the market (see *e.g.* Table I). In order to evaluate the performance of PANDA in this type of measurements, Monte-Carlo simulations of energy scans around the resonance energy have been performed. Events were generated at $N = 10$ different energies around the h_c mass, each point corresponding to 5 days of measurements in the high resolution mode with $\mathcal{L} = 2 \times 10^{31}\mathrm{cm}^{-2}\mathrm{s}^{-1}$. The expected shape of measured resonance in $\bar{p}p \to h_c \to \eta_c\gamma$ is a convolution of the Breit–Wigner resonance curve with the normalized beam energy distribution superimposed on a background. The expected number of events at the i-th data point is:

$$\nu_i = \left[\varepsilon\int\mathcal{L}(t)dt\right]_i \times \left[\sigma_{\mathrm{bkgd}}(E) + \frac{\sigma_p {\mathit{\Gamma}_{\mathrm{R}}}^2/4}{\sqrt{2\pi}\sigma_i} \times \int \frac{\exp-\left[(E-E')^2/2\sigma_i^2\right]}{(E'-M_{\mathrm{R}})^2 + \mathit{\Gamma}_{\mathrm{R}}^2/4} dE'\right], \quad (1)$$

where σ_i is the beam energy resolution at the i-th data point, $\mathit{\Gamma}_{\mathrm{R}}$ and M_{R} are the resonance width and mass, σ_p incorporates branching ratios for the formation and decay, $\sigma_p = 3\pi B_{\bar{p}p} B_{\eta_c\gamma}/k^2$, the factor in square brackets in front of the r.h.s. of Eq. (1) is the product of ε, an overall efficiency and acceptance factor and the integrated luminosity at the i-th data point. The likelihood function, $-\ln L$, assuming Poisson statistics, is minimized to extract the resonance parameters. We assumed signal to background ratio 8:1 and the signal reconstruction efficiency of the $h_c \to \eta_c\gamma \to \phi\phi\gamma$ channel (see Sec. 2.1). The simulated data were fitted to the expected signal shape with the four adjustable parameters: $E_{\mathrm{R}}, \mathit{\Gamma}_{\mathrm{R}}, \sigma_p$, and σ_{bkgd} (assumed energy independent). The study has been repeated for the three different $\mathit{\Gamma}_{\mathrm{R}} = 0.5$, 0.75 and 1.0 MeV. The latter case is illustrated in Fig. 2. We conclude that with the designed parameters of beam energy resolution the measurement of the width of the h_c resonance with about 25% precision is feasible, however the necessity to work with lower luminosity of the high resolution mode leads to a rather time consuming experiment.

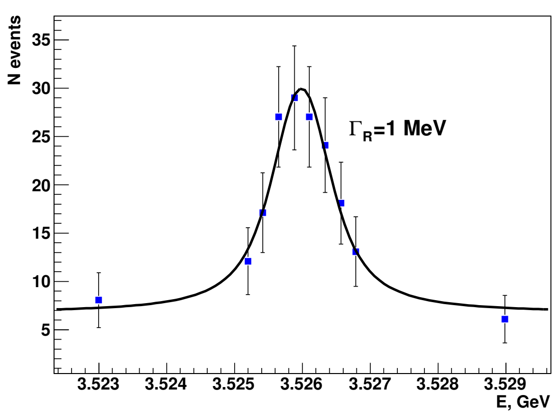

Fig. 2. Fit of the Breit–Wigner distribution convoluted with Gaussian resolution of the beam momentum (Eq. (1), solid line) to the 'experimental points' generated assuming that the h_c width is 1.0 MeV. The fitted width is 0.90 ± 0.22 MeV.

3. Determination of PWO resolution at low gamma-ray energies

The electromagnetic calorimeter (EMC) of PANDA [2] will be built of $PbWO_4$ (PWO) scintillators of 20 cm length, which corresponds approximately to 23 radiation lengths. It has been stressed above that low energy threshold for single photon detection is a desirable feature in the quoted example, which is generally true in the physics program forseen for PANDA (see Ref. [1]). The PANDA Collaboration together with BTCP (Russia), the scintillator producer, made a significant effort to improve quality of PWO, which resulted in much improved light yield of PWO-II in comparison with the pioneer, the CMS detector at CERN [22]. Improvements have been achieved also in PWO readout by applying avalanche photodiodes (APDs) S8664-1010 of Hamamatsu Photonics with the sensitive area 10×10 mm. A further improvement is forseen by cooling EMC down to $-25°$C, which brings about fourfold increase in the emission efficiency compared to room temperature.

Measurements of the achieved resolution as a function of the photon energy have been performed [23] in the 40.9–674.5 MeV range using tagged bremsstrahlung from the MAMI microtron at the University of Mainz. These measurements utilized a 3×3 matrix of $20 \times 20 \times 200$ mm PWO-II scintillators in which the central one was illuminated with a collimated beam of photons and the remaining registered the avalanche photons spreading in the direction transverse to the central's axis. The reduced resolution, σ/E, measured at 16 energies in that range is well approximated with a formula:

$$\sigma/E = 1.31\%/\sqrt{E/\mathrm{GeV}} + 0.65\%\,, \tag{2}$$

in which, the photon energy, E, is expressed in GeV.

Our team designed and constructed a setup intended to measure the resolution at low photon energies to verify validity of Eq. (2) down to energies as close as possible to the forseen single detector threshold. The setup [24] uses a single PWO scintillator and an APD of the same type as in [23]. The crystal is located on the axis of a cylindrical plastic scintillator, covering PWO over almost its total length. The two halves of the plastic register 0.511 MeV annihilation photons emerging from the PWO after the incident photon had been detected in a pair production process. The measurements were performed at 6.13, 12.7 and 17.2 MeV using monoenergetic photons from the $^{11}\mathrm{B}(p,\gamma)^{12}\mathrm{C}$ reaction initiated with 1.92 MeV protons accelerated with the SINS/UW Van-de-Graaff accelerator. The scintillator, APD and preamplifier were cooled down to $-20°$C in these measurements. Our results (points with error bars in Fig. (3)) demonstrate that the dependence established in Ref. [23] in the energy range 40.9–674.5 MeV gives a valid extrapolation of σ/E down to energies close to the EMC detection threshold. It should be stressed that Eq. (2) is corrected for the difference in working temperatures, ours $-20°$C *vs.* $0°$C in that work.

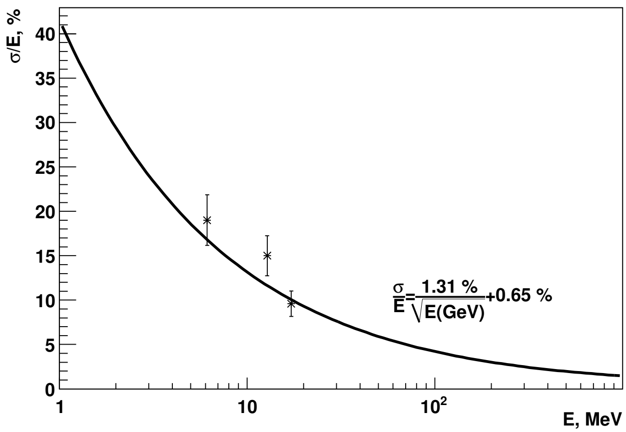

Fig. 3. Reduced Gaussian resolution, σ/E, measured at the three photon energies mentioned in the text (points with error bars) compared with the smooth energy dependence, Eq. (2), established in Ref. [23] (solid line).

We are happy to acknowledge the assistance of the staff of the Sołtan Institute in carrying out this work, which represents part of the PhD Thesis of the first author (D.M.). This work was supported in part by the European Community Framework Program FP6 under the contracts RII3-CT-2003-506078; Hadron Physics and 515873 DIRACsecondary-Beams; PANDA 4. This work received also support on behalf of the Polish Ministry for Science and Higher Education and the International Post-Graduate Studies of the Polish Academy of Sciences.

REFERENCES

[1] The PANDA Collaboration, `http://www-panda.gsi.de/archive/public/panda_pb.pdf` (2009).

[2] The PANDA Collaboration, `http://www-panda.gsi.de/archive/public/panda_tdr_EMC.pdf` (2008).

[3] C. Amsler *et al.*, *Phys. Lett.* **B667**, 1 (2008).

[4] E.S. Swanson, *Phys. Rep.* **429**, 243 (2006).

[5] F.M. Renard, *Phys. Lett.* **B65**, 157 (1976).

[6] V.A. Novikov *et al.*, *Phys. Rep.* **41**, 1 (1978).

[7] R. McClary, N. Byers, *Phys. Rev.* **D28**, 1692 (1983).

[8] Y.P. Kuang, S.F. Tuan, T.M. Yan, *Phys. Rev.* **D37**, 1210 (1988).

[9] M. Chemtob, H. Navelet, *Phys. Rev.* **D41**, 2187 (1990).

[10] V.O. Galkin *et al.*, *Sov. J. Nucl. Phys.* **51**, 705 (1990).

[11] G.T. Bodwin, E. Braaten, G.P. Lepage, *Phys. Rev.* **D46**, 1914 (1992).

[12] R. Casalbuoni *et al.*, *Phys. Lett.* **B302**, 95 (1993).

[13] K.T. Chao, Y.B. Ding, D.H. Qin, *Phys. Lett.* **B301**, 282 (1993).

[14] G.P. Chen, Y.P. Yi, *Phys. Rev.* **D46**, 2918 (1992).

[15] P. Ko, *Phys. Rev.* **D47**, 2837 (1993).

[16] S.N. Gupta *et al.*, *Phys. Rev.* **D49**, 1551 (1994)

[17] M. Suzuki, *Phys. Rev.* **D66**, 037503 (2002).

[18] T. Lähde, *Nucl. Phys.* **A714**, 183 (2003).

[19] T. Barnes, S. Godfrey, E.S. Swanson, *Phys. Rev.* **D72**, 054026 (2005).

[20] J.J. Dudek, R.G. Edwards, D.G. Richards, *Phys. Rev.* **D73**, 074507 (2006).

[21] F. De Fazio, *Phys. Rev.* **D79**, 054015 (2009).

[22] The CMS Collaboration, CMS: The Electromagnetic Calorimeter, Technical Design Report, CERN-LHCC-97-33 (1997).

[23] R.W. Novotny *et al.*, *IEEE Trans. Nucl. Sci.* **55**, 1295 (2008).

[24] D. Melnychuk *et al.*, *Nucl. Instrum. Methods* **A607**, 600 (2009).